STM JOURNALS

Journal of
Polymer & Composites

ISSN: 2321-2810 (Online)
ISSN: 2321-8525 (Print)
Volume 13, Issue 5, 2025
DOI (Journal): 10.37591/JoPC

https://journals.stmjournals.com/jopc/

Research JoPC

# Thermal Conductivity and Energy Storage Performance of Paraffin Wax-Based Composites Reinforced with Amine Functionalized Graphene as a Nanofiller

Daya Shankar Prasad[1,*], Pradeep Kumar Singh[2]

***Abstract***

*In this study, amine-functionalized graphene (AFG) was employed as a nanofiller/nanomaterial to enhance the thermal and structural properties of a paraffin wax (PW)-based polymeric composite, formulated as a phase change material (PCM). The PW/AFG composite was synthesized with varying nanofiller volume fractions (0.20%, 0.40%, 0.80%, and 1.60%), and its thermal conductivity, stability, and energy storage performance were systematically analyzed. The incorporation of AFG into the polymer matrix significantly improved the composite's thermal conductivity, achieving enhancements of 13.58% to 46.42%. The experimental results confirmed the duration of composite charging time reduced by 61.5% and discharging time extended by 62.5% with increasing the concentration of nanofiller in PW. The rheological and morphological behavior of the composites was also studied to understand filler-matrix interactions. The composite exhibited enhanced thermal stability and latent heat storage, confirming effective dispersion and compatibility of AFG within the paraffin matrix. It has been observed that the optimal concentration is 0.8 vol% based on a comparative analysis of thermal conductivity, charging/discharging times, and stability across various concentrations. These results highlight the potential of polymer-based composite PCMs for advanced thermal energy storage applications.*

**Keywords:** Nanocomposite; polymer; phase change material (PCM); amine-functionalized graphene; thermal stability

## INTRODUCTION

Phase change materials (PCMs) have garnered significant attention for thermal energy storage due to their ability to absorb, store, and release large quantities of latent heat during phase transitions. These materials are widely recognized for their cost-effectiveness and high latent heat capacity, which enhance the efficiency and versatility of energy storage systems. However, pure PCMs such as PW suffer from limitations, particularly low thermal conductivity and sensitivity to rapid thermal loads during charging and discharging cycles, which can hinder system performance and energy efficiency [1].

To address these challenges, researchers have explored the incorporation of nanoparticles into PCMs, forming nanocomposite structures that improve thermal conductivity and mechanical integrity [2–4]. Among the various enhancement techniques, the use of high-thermal-conductivity nanomaterials such as graphene, carbon nanotubes, and metal oxides has been shown to significantly boost the heat transfer performance of PCMs. Additional strategies, including the integration of fins and heat pipes, have also been proposed to improve thermal behaviour [5, 6].

***Author for Correspondence**
Daya Shankar Prasad
E-mail: dspbgiet@gmail.com

[1]Research Scholar, Department of Mechanical Engineering, GLA University, Mathura, Uttar Pradesh, India
[1]Assistant Professor, Department of Mechanical Engineering, MVN University, Palwal, Haryana, India
[2]Assistant Professor, Department of Mechanical Engineering, GLA University, Mathura, Uttar Pradesh, India

Received Date: July 09, 2025
Accepted Date: August 12, 2025
Published Date: August 28, 2025

**Citation:** Daya Shankar Prasad, Pradeep Kumar Singh. Thermal Conductivity and Energy Storage Performance of Paraffin Wax-Based Composites Reinforced with Amine Functionalized Graphene as a Nanofiller. Journal of Polymer & Composites. 2025; 13(5): 355–374p.

 

PCMs are utilized across a range of applications, including thermal energy storage, building insulation, solar heating systems, and thermal regulation of electronic devices. They are generally categorized into organic, inorganic, and eutectic types. Organic PCMs, such as PW and fatty acids, are valued for their chemical stability, compatibility, and minimal phase separation, whereas inorganic PCMs, such as salt hydrates and metals, offer higher thermal conductivity but may suffer from supercooling, corrosion, and phase segregation [7, 8].

PW stands out as a widely used organic polymer-based PCM due to its high latent heat, chemical stability, availability, and cost-effectiveness [9, 10]. Its favourable melting point range makes it adaptable to various thermal storage applications. Furthermore, PW demonstrates good compatibility with nanomaterials, particularly carbon-based fillers, which can significantly improve its thermal conductivity and performance when formulated as a polymer nanocomposite.

Thermal energy storage systems (TESS) play a critical role in managing renewable energy, recovering waste heat, and stabilizing energy supply. TESS operates on three storage mechanisms: sensible heat storage (SHS), latent heat storage (LHS), and thermochemical heat storage (TCHS) [11, 12]. Among these, LHS using PCMs is particularly effective due to its high energy density and ability to maintain near-constant temperature during thermal cycling [13]. Recent studies have highlighted that latent heat storage systems (LHSS) can be optimized through both material-level enhancements and system-level designs, improving heat transfer rates, energy efficiency, and long-term operational stability [14, 15].

Among PCM types, paraffin-based materials are preferred for their excellent latent heat properties, chemical inertness, low corrosiveness, and negligible volume change during phase transitions, which supports dimensional and structural integrity [11]. Their adaptability across applications and compatibility with nanofillers especially functionalized carbon nanomaterials makes them ideal candidates for advanced polymeric nanocomposite PCMs.

The integration of carbon-based nanomaterials into PCMs has emerged as a promising strategy to significantly enhance their thermal conductivity and overall energy storage performance. Prasad et al. [16] demonstrated that the incorporation of amine-functionalized multi-walled carbon nanotubes (MWCNTs) into PW improved thermal conductivity by 34.33%, enhancing its efficiency for thermal energy storage (TES) applications. Similarly, He et al. [17] investigated PEG/graphene nanoplatelet (GNP) composites and reported a substantial increase in thermal conductivity at 1.5 wt% GNP loading, along with excellent photo-thermal conversion efficiency and improved thermal stability.

Khezri et al. [18] enhanced microencapsulated PCMs by embedding GNPs, achieving a 93% increase in thermal diffusivity and a 48% rise in thermal conductivity, while preserving latent heat and structural stability essential attributes of functional composite materials. Sun et al. [11] further explored nano-graphite and coconut-shell-based carbon additives in paraffin and noted improved melting characteristics at low concentrations, though agglomeration at higher concentrations diminished performance.

Graphene-based additives consistently exhibit enhanced thermal conductivity. Nagar et al. [19] reported improved charging behaviour in PW-graphene composites, while Nair et al. [20] established that myristic acid-based PCMs with high heat transfer rates suit rapid-response applications. This emphasizes the necessity of customizing PCM selection according to the thermal response demands of the intended application.

Kanimozhi et al. [21] optimized the thermal performance of paraffin-based PCMs by embedding multiple copper tubes and varying fluid flow rates, confirming superior heat retention. Rao and Liu [22] compared graphene and exfoliated graphite sheets (EGS) in paraffin systems, finding that graphene produced better thermal performance. Interestingly, enthalpy initially increased with filler loading before decreasing, suggesting a complex interplay between filler content and heat storage capability.

 

Functionalized graphene variants have also been studied. Kumar et al. [23] used carboxyl-functionalized graphene, achieving up to a 50% thermal conductivity improvement and a 35% reduction in charging time. Pan et al. [24] and Sharma et al. [25] both demonstrated that graphene oxide (GO) enhanced thermal performance in paraffin, with reductions in charging/discharging times up to 40% and thermal conductivity improvements up to 60%, depending on concentration and heat transfer fluid (HTF) flow rate.

Further, Zhao et al. [26] introduced graphene-stabilized Pickering emulsions to form microencapsulated PCMs (MPCMs), demonstrating improved phase stability and heat retention. Hussain et al. [27] applied graphene-coated nickel foams with PCMs for lithium-ion battery cooling, reducing maximum cell temperatures by 15°C, enhancing both battery lifespan and thermal regulation.

Other studies, such as Nagar et al. [28], confirmed that carboxyl-functionalized graphene significantly reduced PCM charging times (up to 38%) by enhancing thermal conductivity. Viswanathan et al. [29] employed $Al_2O_3$ nanoparticles to improve PCM behavior in electric vehicle applications. Similarly, Lin et al. [30] showed that expanded graphite (3 wt%) could increase storage efficiency by over 40%. Hybrid nanomaterials such as CuO-MWCNT and CNT-graphene composites have also demonstrated synergistic effects, improving both conductivity and phase transition rates [31, 32].

A broader review by Mishra et al. [33] reinforced that carbon-based additives like graphene and CNTs are particularly effective in improving PCM performance. Shape-stable PCM composites such as beeswax–carbon hybrids [34] have also shown promise in preventing leakage while maintaining thermal efficiency. Mayilvelnathan and Arasu [35] demonstrated that 1 wt% graphene added to erythritol led to a 21% reduction in melting time and 30% enhancement in heat transfer efficiency in a shell-and-tube thermal energy system.

Collectively, these studies underscore the crucial role of carbon-based nanofillers in enhancing the thermal properties of polymer-based PCM composites for energy storage systems. Nanomaterial incorporation especially, functionalized graphene has proven highly effective in improving filler dispersion, interfacial bonding, thermal conductivity, and heat storage stability.

Despite extensive study, research, and publication have been done so far for improving the TESS charging & discharging processes by using various nanomaterials, including graphene but by the addition of AFG (amine-functionalized graphene) into PCM is a state of arts in this regard.

Furthermore, systematic analysis of both AFG concentration and HTF flow rate on charging/discharging dynamics remains limited in the literature.

Therefore, this study aims to investigate the thermal behaviour and performance of AFG reinforced paraffin-based nanocomposite PCMs under varying concentrations and HTF flow rates. The experimental findings provide insights into the structure–property relationships of these composite materials and their potential for scalable TES applications.

## EXPERIMENTAL PROCEDURE

### Materials Selection and Preparation of Composite

In this study, PW was selected as the base PCM owing to its favourable latent heat storage capacity, chemical stability, and compatibility with nanofillers. The PW was procured from Eco-sense Sustainable solutions Pvt. Ltd., Okhla, India. AFG, used as a thermal conductivity-enhancing nanofiller, was supplied by Platonic Nanotech Pvt. Ltd., India.

According to the supplier's technical data sheet, the $NH_2$-G was produced by a modified Hummer's method followed by proprietary amine functionalization. The resulting material is a fluffy, grey-black powder with >99% purity, 1–5 nm thickness, 5–10 μm flake length, an average of 4–8 graphene layers,

 

and a surface area of 190–220 m²/g. The nitrogen content is 6% with an amine group ratio of 10–15 wt%, which facilitates enhanced compatibility with organic matrices such as paraffin wax by promoting hydrogen bonding and interfacial adhesion, thereby reducing filler agglomeration.

To prepare the nanocomposites, AFG was reinforced into the molten PW at volume fractions of 0.20%, 0.40%, 0.80%, and 1.60%. Each mixture was subjected to a controlled ultrasonication process to achieve homogenous dispersion of the nanofiller within the polymer matrix, thereby ensuring optimal interfacial bonding and minimizing agglomeration (Figure 1). The sonication enhances filler distribution and maximizes surface interaction between the AFG and the paraffin matrix.

**Characteristics of Materials**

The thermophysical properties of both PW and AFG are critical in determining their suitability for thermal energy storage applications. Tables 1 and 2 summarize their essential characteristics for various applications

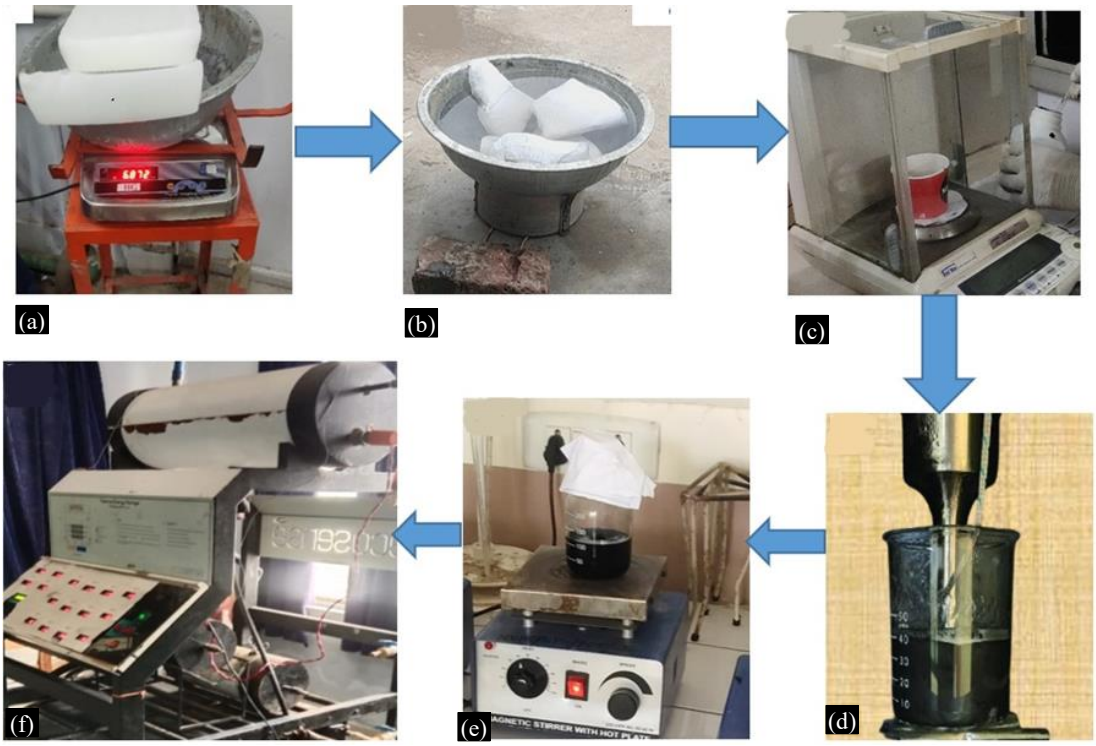


**Figure 1.** Composite preparation to experimentation: (a) Weighing of PW to ensure precise measurements, (b) Melting of PW to achieve a uniform molten state, (c) Weighing the required amount of nanomaterial accurately, (d) Sonication process to ensure proper dispersion of the nanomaterial, (e) Sample preparation to obtain the desired composition and structure, (f) Setup for Experimental performance analysis.

**Table 1.** Characteristics of PCM.

| PCM type | Organic (PW) |
|---|---|
| Thermal Conductivity (Liquid State) | 0.167 (W/m K) |
| Thermal Conductivity (Solid State) | 0.346 (W/m K) |
| Density (Liquid State) | 790 (kg/m$^3$) |
| Density (Solid State) | 916 (kg/m$^3$) |
| Specific Heat Capacity (Liquid State) | 2.14 (kJ/kg K) |
| Solid State Specific Heat Capacity | 2.9 (kJ/kg K) |
| Latent Heat of Fusion | ~175 (KJ/kg) |
| Fusion Temperature | 55-62 (°C) |

 

**Table 2.** Characteristics of graphene.

| **Graphene** | **Amine (-$NH_2$) groups** |
|---|---|
| Purity | Approximately 99% |
| Graphene Thickness | 1-5 nm |
| Graphene Length | 5-10 micron |
| Avg. No. of Layer | 4-8 |
| Amine Ratio | 10-15 wt% |
| Aspect ratio | Extremely high |
| Surface Area | 190-220 $m^2/g$ |

These properties are fundamental in tailoring the thermal conductivity and phase change characteristics of the resulting nanocomposite for practical energy storage applications.

## Experimental Setup and Instrumentation

A laboratory experimental setup was established to assess the thermal charging and discharging behaviour of both pure PW and AFG-reinforced PW composites. The actual laboratory setup and its schematic layout are shown in Figures 2 and 3, respectively. The actual laboratory setup was procured from ECOSENSE Sustainable Pvt. Ltd., New Delhi, India.

The setup includes a 5.5 kg cylindrical PCM container connected to two insulated tanks-one for hot and one for cold HTF. Each tank has a capacity of 120 liters. The HTF is circulated using a 0.12 HP centrifugal pump (max. flow rate: 33 LPM), and heated via two 1500 W immersion heaters installed in the hot water tank. A 50-liter intermediate tank is used to collect and deliver HTF during charging and discharging. Essential parameters, such as the inlet and outlet temperatures of the PCM and HTF, along with the temperature of the storage tanks, were continuously tracked and logged through the control panel. The experiment was carried out for both thermal charging as well as thermal discharging processes to evaluate the performance of the PCM cylinder (PCM unit). Class-A temperature sensors (sensing range: –200 to 650 °C) were utilized for temperature measurement, while a stopwatch was used for recording the thermal response times.

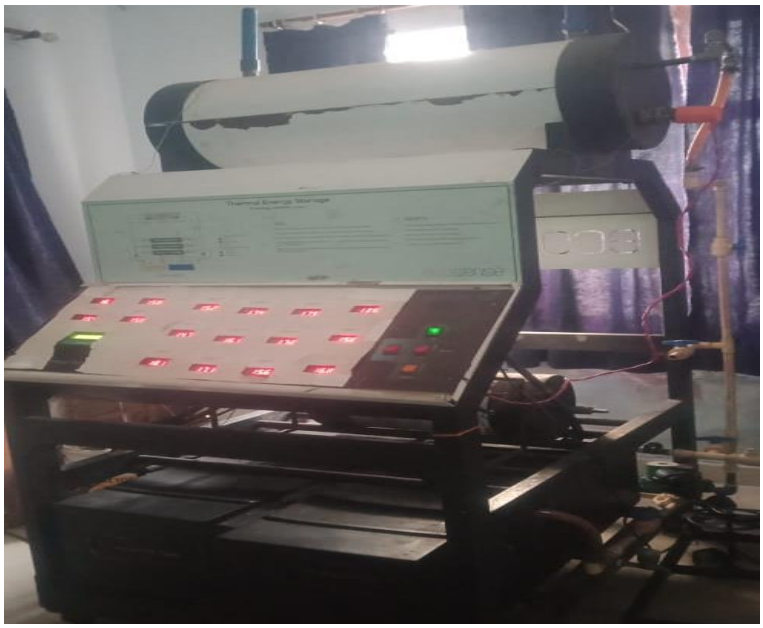

**Figure 2.** Actual laboratory setup of the TES system showing the cylindrical PCM container, hot and cold-water storage tanks (120 L each), intermediate tank (50 L), centrifugal pump, immersion heaters, control panel, and associated piping and instrumentation.

 

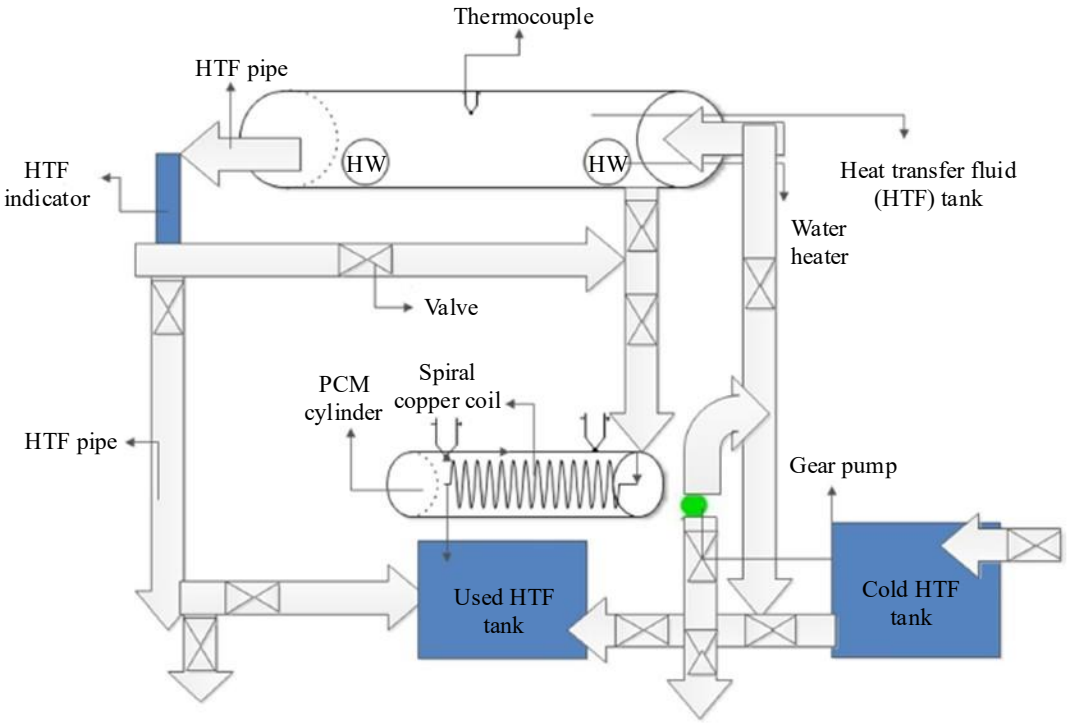


**Figure 3.** Schematic diagram of the TES experimental setup illustrating the hot and cold-water tanks, PCM storage unit, centrifugal pump, intermediate tank, immersion heaters, temperature sensors, and piping layout for charging and discharging processes [23].

**Evaluation of Thermal Performance of the Composite PCM**

The thermal behaviour of the PCM cylinder was assessed through sequential charging and discharging cycles. During charging, heated HTF (~82–85 °C) was pumped from the hot tank into the PCM unit. Heat was transferred to the PCM composite, triggering the solid–liquid phase transition. The process was deemed complete when the outlet temperature of the PCM unit stabilized at ~60 °C, indicating complete of charging process.

During the discharging process, cool water was circulated from the cold storage tank through the PCM cylinder. The solidification of the PCM released stored latent heat to the HTF, which was then returned to the cold tank. This process continued until the outlet temperature approached room temperature, completing the discharging cycle.

The influence of AFG concentration and HTF flow rate on thermal response time was studied systematically. These experiments helped quantify the impact of nanofiller incorporation on thermal conductivity, energy retention, and overall composite PCM performance.

## RESULTS AND DISCUSSION

The experimental investigation was conducted to analyze the effect of AFG reinforcement on the thermal performance of PW, a polymer-based phase change material. Various concentrations (0.20%, 0.40%, 0.80%, and 1.60% by volume) of AFG were studied at different HTF flow rates (6.25, 12.5, and 25 ml/sec). Results were interpreted through thermal performance data, Field emission scanning electron microscopy (FESEM) analysis, thermal conductivity measurements (by TPS method), Thermogravimetric Analysis (TGA), and Differential Scanning Calorimetry (DSC). Also, for supporting the presence of amine functional groups and their role in enhancing compatibility between graphene and paraffin wax, Fourier Transform Infrared Spectroscopy (FTIR) analysis of AFG was performed.

 

**Thermal Performance during Charging Process**

The thermal charging process involves the absorption of heat by the PCM from the HTF, leading to a phase transition from solid to liquid. The efficiency and rate of this thermal energy absorption are primarily governed by the PCM's thermal conductivity and the flow characteristics of the HTF.

To overcome the inherently low thermal conductivity of PW, AFG a high thermal conductivity nanomaterial-was incorporated into PW at varying concentrations. This modification aimed to facilitate improved heat transfer pathways within the PCM matrix, thereby reducing the overall charging duration and enhancing system performance.

The following subsections present and discuss the thermal charging characteristics of both pure PW and AFG-reinforced PW were experimentally analysed under varying volumetric concentrations of AFG (0.20%, 0.40%, 0.80%, and 1.60%) and at multiple HTF flow rates (6.25, 12.5, and 25 ml/sec). The influence of AFG on thermal conductivity and its role in accelerating the melting process were systematically evaluated to determine its effect on energy storage performance.

***Effect of AFG concentration on thermal charging at 6.25 ml/sec***

The thermal charging behaviour of PW and AFG-based PW at a flow rate of 6.25 ml/sec is depicted in Figure 4. Pure PW exhibited the longest charging duration, requiring approximately 160 minutes to achieve complete melting. This extended duration is attributed to its inherently low thermal conductivity, which limits the rate of heat transfer from the HTF to the PCM.

Incorporating AFG into the PW matrix led to a significant reduction in charging time, with higher AFG concentrations yielding better thermal performance. At 0.20 vol%, the charging time was reduced to 110 minutes, a 31.25% improvement over pure PW. Increasing the concentration to 0.40 vol% further decreased the charging duration to 90 minutes, representing a 43.75% reduction. The most notable improvement was observed at 0.80 vol%, where the charging time dropped to 80 minutes, marking a 50% reduction [16, 29–31].

However, at 1.60 vol%, no additional reduction in charging time was observed, with the charging duration remaining at 80 minutes. This saturation effect suggests that beyond 0.80 vol%, the thermal conductivity gains are offset by nanoparticle agglomeration, which creates thermal resistance and hinders effective heat dispersion within the PCM matrix [16, 29].

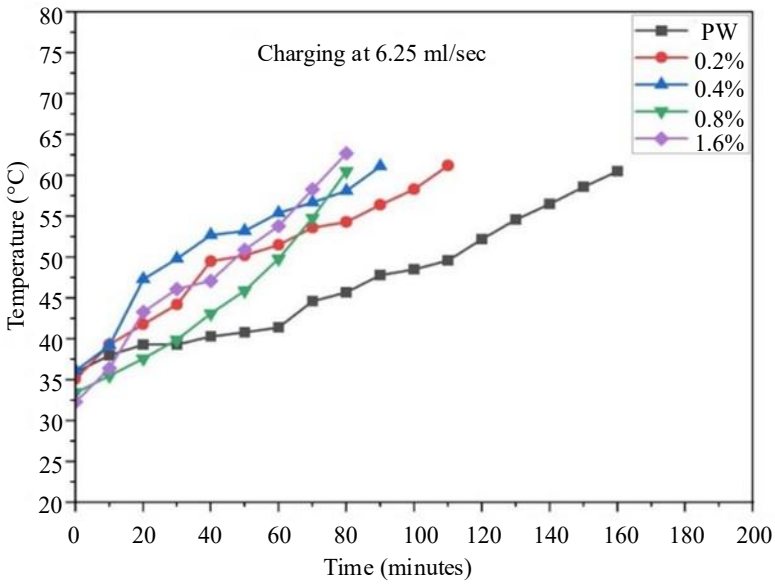


**Figure 4.** Thermal charging of PW and AFG-based PW composites at 6.25 ml/sec.

 

These findings confirm that AFG significantly improves the thermal charging behaviour of PW by enhancing its thermal conductivity and reducing the overall heat transfer resistance. However, there exists an optimal concentration, around 0.80 vol%-beyond which performance gains plateau due to dispersion limitations.

***Effect of AFG concentration on thermal charging at 12.5 ml/sec***

The thermal charging performance of pure PW and its AFG-enhanced composites at a flow rate of 12.5 ml/sec is presented in fig. 5. The data show a general reduction in charging time with increased HTF flow rate, which promotes improved convective heat transfer. At this flow rate, the charging time for pure PW reduced to 150 minutes-10 minutes less than the 6.25 ml/sec case -demonstrating the beneficial effect due to increased flow rates on thermal performance.

With the incorporation of AFG, the thermal response improved significantly. A 0.20 vol% addition of AFG reduced the charging time to 80 minutes, corresponding to a 46.67% improvement relative to pure PW. Increasing the concentration to 0.40 vol% further decreased the charging duration to 70 minutes (53.3% reduction), while 0.80 vol% resulted in the most efficient charging behaviour, achieving complete melting in just 60 minutes-a 60% reduction in charging time [16, 29–31].

Interestingly, at 1.60 vol% AFG, the charging time increased to 120 minutes, deviating from the previously observed trend. This increase is likely attributed to nanoparticle agglomeration, which impairs uniform heat distribution and reduces effective thermal conductivity [16, 29]. Such clustering can form localized thermal resistances, offsetting the benefits of enhanced conduction.

Overall, the results indicate an optimal AFG concentration of approximately 0.80 vol%, beyond which the thermal performance of the PCM composite begins to deteriorate due to dispersion challenges.

***Effect of AFG concentration on thermal charging at 25 ml/sec***

The impact of AFG concentration on the thermal charging behaviour of PW at a flow rate of 25 ml/sec is presented in Figure 6. As expected, increasing the flow rate improves convective heat transfer, resulting in a shorter charging time. Pure PW exhibited a charging duration of 130 minutes at this flow rate, which is 10 minutes shorter than at 12.5 ml/sec and 30 minutes less than at 6.25 ml/sec, indicating a consistent trend of enhanced thermal charging performance with increased HTF flow rate.

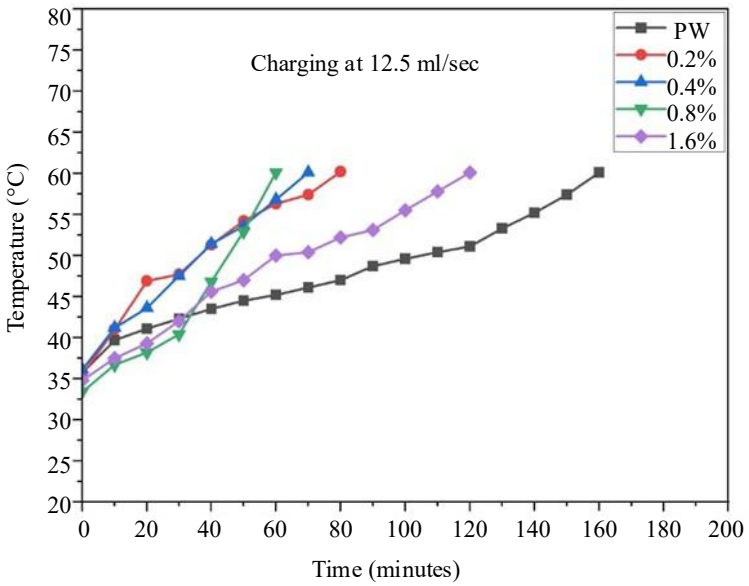


**Figure 5.** Thermal Charging of PW and AFG-Based PW Composites at 12.5 ml/sec.

 

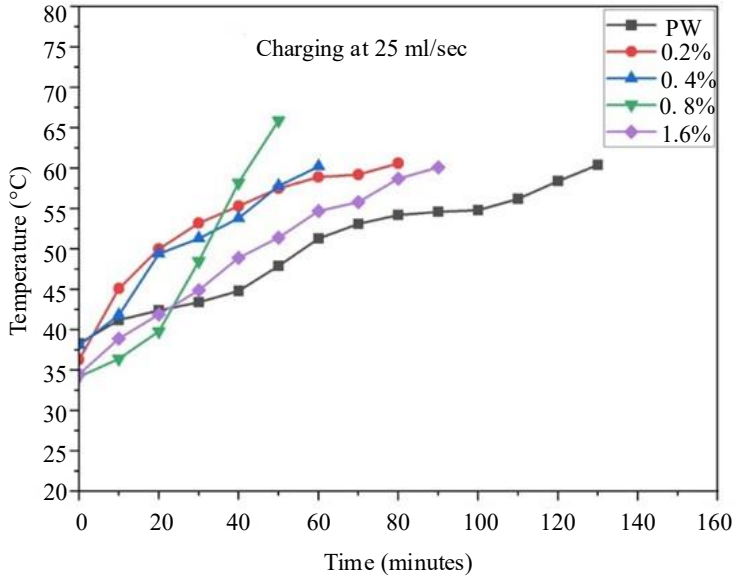


**Figure 6.** Thermal charging of PW and AFG-based PW composites at 25 ml/sec.

The incorporation of AFG significantly improved thermal performance. At 0.20 vol%, the charging time was reduced to 80 minutes, indicating a 38.46% decrease compared to pure PW. Increasing the concentration to 0.40 vol% further reduced the charging time to 60 minutes, amounting to a 58.85% improvement. The most pronounced effect was observed at 0.80 vol%, where the composite required only 50 minutes to complete the charging process-marking a 61.5% reduction in charging duration [16, 29–31].

However, further increasing the AFG content to 1.60 vol% resulted in an unexpected increase in charging time to 90 minutes. This deviation is attributed to nanoparticle agglomeration at higher concentrations, which can inhibit uniform dispersion and impair heat conduction pathways [16, 29]. Such aggregation can introduce localized thermal resistances in the composite, ultimately reducing the performance of heat transfer despite the higher nanomaterial concentration.

These results emphasize that both flow rate and nanoparticle concentration critically affect the thermal charging behaviour of PCM composites. Increasing the flow rate from lower to higher significantly reduces the charging time due to improvement of heat transfer. The addition of AFG further increases thermal conductivity, facilitating faster heat absorption. However, when the concentration goes beyond 0.80 vol%, the improvement in performance decreases due to microstructural limitations and doesn't allow heat to flow efficiently.

**Thermal Performance during Discharging Process**

The discharging phase in a TESS is as important as the charging phase, as it determines how effectively the stored heat can be utilised. During discharging, the PCM transfers the stored heat to the HTF, typically water, as the PCM cools down and changes from liquid back to solid.

Both the HTF flow rate and the concentration of the nanomaterial (AFG) have a strong influence on the discharging process. These parameters affect the heat transfer rate by altering the thermal conductivity and convective heat exchange of the PCM composite.

The following subsections present and discuss the experimental results for the discharging performance of PW and AFG-based PW composites at various AFG concentrations (0.20, 0.40, 0.80, and 1.60 vol%) and different HTF flow rates (6.25, 12.5, and 25 ml/sec).

 

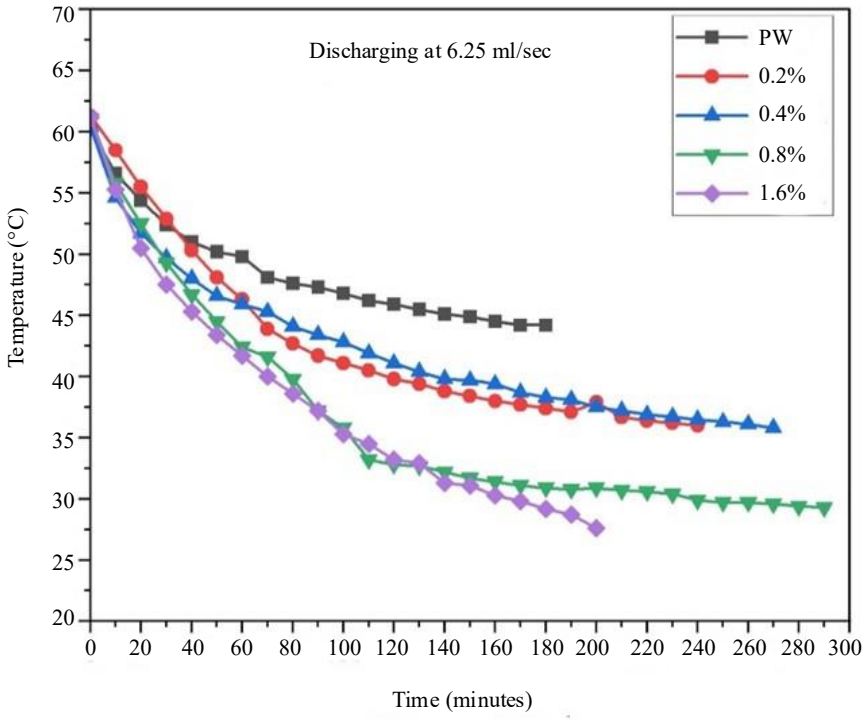


**Figure 7.** Thermal discharging of PW and AFG-based PW composites at 6.25 ml/sec.

***Effect of AFG on thermal discharging at 6.25 ml/sec***

Figure 7 illustrates the thermal discharging behaviour of PW and AFG-based PW composites at HTF flow rate of 6.25 ml/sec. The results show that pure PW discharges the fastest, completing the process in about 180 minutes. As the concentration of AFG increases, the discharging time becomes longer. For instance, the addition of 0.20 vol% AFG extends the discharging time to 240 minutes (an increase of 33.33%), while 0.40 vol% extends it to 270 minutes (50% rise). The longest discharging time, 290 minutes, is observed with 0.80 vol% AFG-about a 61.1% increase compared to pure PW [16, 31].

Interestingly, when the AFG concentration is further increased to 1.60 vol%, the discharging time drops to 200 minutes, which is 11.1% longer than pure PW but shorter than the times observed at intermediate concentrations (0.20–0.80 vol%). This trend suggests a nonlinear relationship between AFG content and discharging performance.

At lower concentrations (0.20–0.80 vol%), the nanomaterial likely enhances the heat retention capacity of the PCM, which delays heat release and extends the discharging time. However, at higher concentration (1.60 vol%), the possible aggregation of AFG particles in the composite matrix may form efficient thermal conduction paths, leading to quicker heat transfer and a shorter discharging time despite the higher nanomaterial concentration [16].

***Effect of AFG on thermal discharging at 12.5 ml/sec***

Figure 8 shows the discharging behaviour of PW and AFG-enhanced composites at a flow rate of 12.5 ml/sec. At this flow rate, pure PW exhibits the shortest discharging time, completing the heat release in approximately 160 minutes. As the AFG concentration increases, the discharging time also increases. Specifically, the composite with 0.20 vol% AFG extends the discharging period to 230 minutes (a 43.75% increase), while 0.40 vol% and 0.80 vol% result in discharging times of 240 minutes (50% rise) and 260 minutes (62.5% rise), respectively.

However, a notable shift occurs at 1.60 vol% AFG, where the discharging time decreases to 150 minutes, which is 6.25% shorter than that of pure PW. This shift suggests a transition in behaviour of composite at higher concentrations of AFG.

 

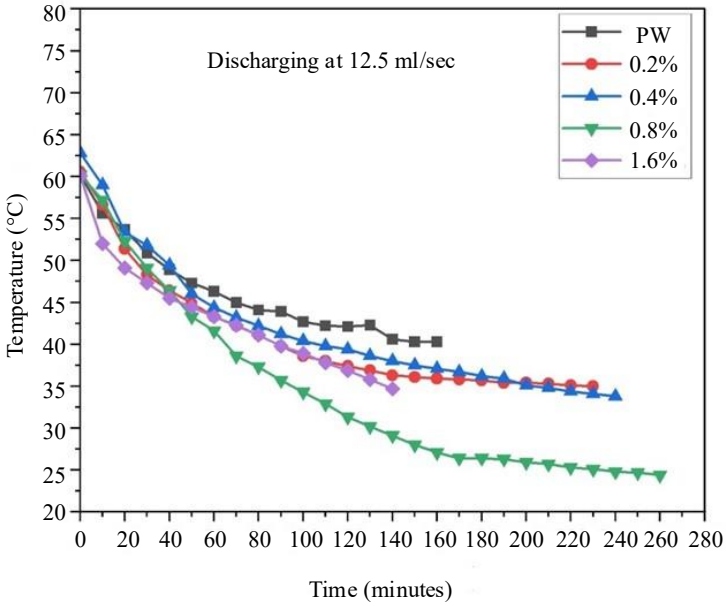


**Figure 8.** Thermal discharging of PW and AFG- based PW composites at 12.5 ml/sec.

At lower concentrations (0.20%–0.80%), the nanomaterial appears to enhance the thermal storage capacity, leading to a slower release of stored energy and consequently longer discharging times [16, 31]. In contrast, at 1.60 vol%, the effect of increased thermal conductivity becomes dominant. Likely due to nanoparticle aggregation, thermal pathways improve, enabling faster heat transfer and thus reducing the discharging time.

Figure 8 clearly demonstrates a nonlinear relationship between AFG concentration and discharging behaviour. The longest discharging time is observed at 0.80 vol%, beyond which a marked reduction is recorded at 1.60 vol%, emphasizing the importance of nanoparticle distribution and concentration in governing the PCM's thermal performance.

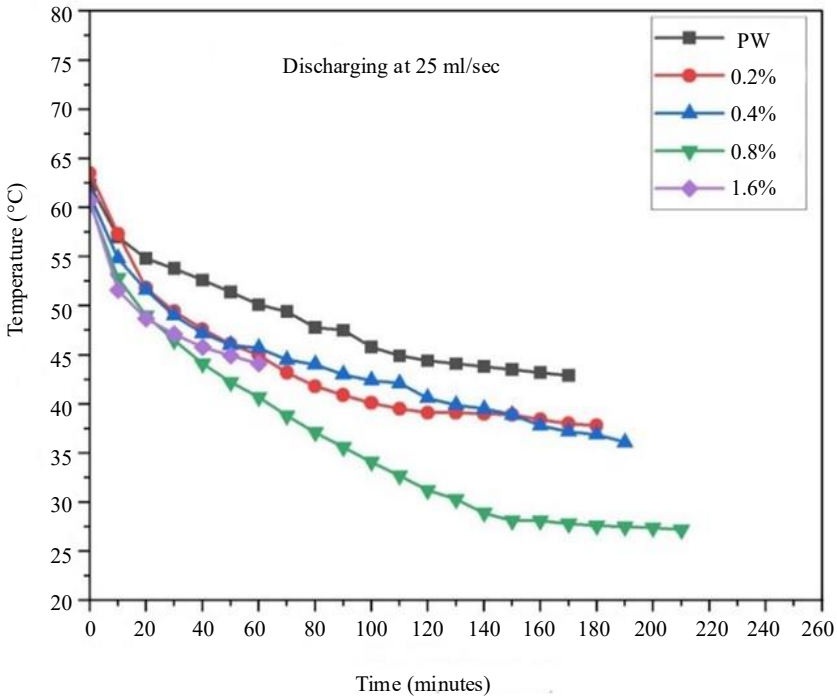


**Figure 9.** Thermal discharging of PW and AFG- based PW composites at 25 ml/sec.

 

***Effect of AFG on thermal discharging at 25 ml/sec***

Figure 9 illustrates the discharging characteristics of PW and AFG-based PW composites at a flow rate of 25 ml/sec. Pure PW shows the shortest discharging time, completing the process in 170 minutes. As the concentration of AFG increases, a gradual rise in discharging duration is observed: 180 minutes for 0.20 vol% (5.9% increase), 190 minutes for 0.40 vol% (11.8% increase), and 210 minutes for 0.80 vol% (23.52% increase). Notably, at 1.60 vol% AFG, the discharging time significantly drops to just 60 minutes, representing a 64.7% reduction compared to pure PW [16].

This behaviour highlights the dual influence of AFG on thermal storage and heat release performance. At lower concentrations (0.20%–0.80%), AFG appears to improve the heat retention capacity of PW, thereby prolonging the discharging time due to slower heat transfer [16, 31]. However, at higher concentration (1.60 vol%), enhanced thermal conductivity becomes the dominant factor. Likely caused by nanoparticle agglomeration, this forms efficient thermal pathways that accelerate the heat dissipation process.

Figure 9 confirms a nonlinear trend between AFG content and discharging behaviour. The longest discharging time is recorded at 0.80 vol%, followed by a sharp reduction at 1.60 vol%. This finding underscores the critical role of nanoparticle dispersion in altering the thermal performance of PW-based PCMs.

Overall, AFG concentration and flow rate of HTF play crucial roles in determining the thermal performance of the composite PCM. Higher flow rates enhance convective heat transfer, reducing charging and discharging times, whereas lower flow rates allow thermal storage effects to dominate, extending charging and discharging durations. An optimal concentration of 0.80 vol% AFG provides the most effective balance between reduced charging time and extended discharging duration, establishing it as a promising candidate for efficient thermal energy storage applications.

**FESEM Analysis of AFG-based PW Composites**

FESEM was performed to investigate the microstructural characteristics of pure PW and $NH_2$-functionalized graphene reinforced PW composites at different concentrations. The corresponding images are presented in Figure 10.

Figure 10(a) displays the microstructure of pure PW, which exhibits a smooth and continuous surface morphology, devoid of visible defects such as cracks or voids. This homogeneous structure is typical of PW and is indicative of its low thermal conductivity, as the heat transfer mechanism is primarily limited to phonon transport within the unmodified wax matrix.

In contrast, the incorporation of AFG alters the microstructure significantly, as seen in Figures. 10(b)–10(e). At 0.20 vol% AFG (Figure 10b), the surface becomes slightly rougher, and the distribution appears relatively uniform, suggesting good dispersion of nanofillers within the polymer matrix. As the concentration increases to 0.40 vol% and 0.80 vol% (Figures. 10c and 10d, respectively), the presence of layered and interlinked structures becomes more prominent, confirming improved interfacial interactions and effective embedding of AFG within the PW matrix. This enhancement in surface roughness and structural complexity is expected to facilitate better heat conduction pathways through the composite.

However, at 1.60 vol% AFG (Figure 10e), signs of particle agglomeration become evident. These clusters may act as thermal bottlenecks, disrupt the continuous thermal network and potentially reduce the composite's effective thermal conductivity. Despite this, the overall analysis confirms the successful integration of AFG within the PW matrix and reveals a critical relationship between filler concentration and structural morphology.

 

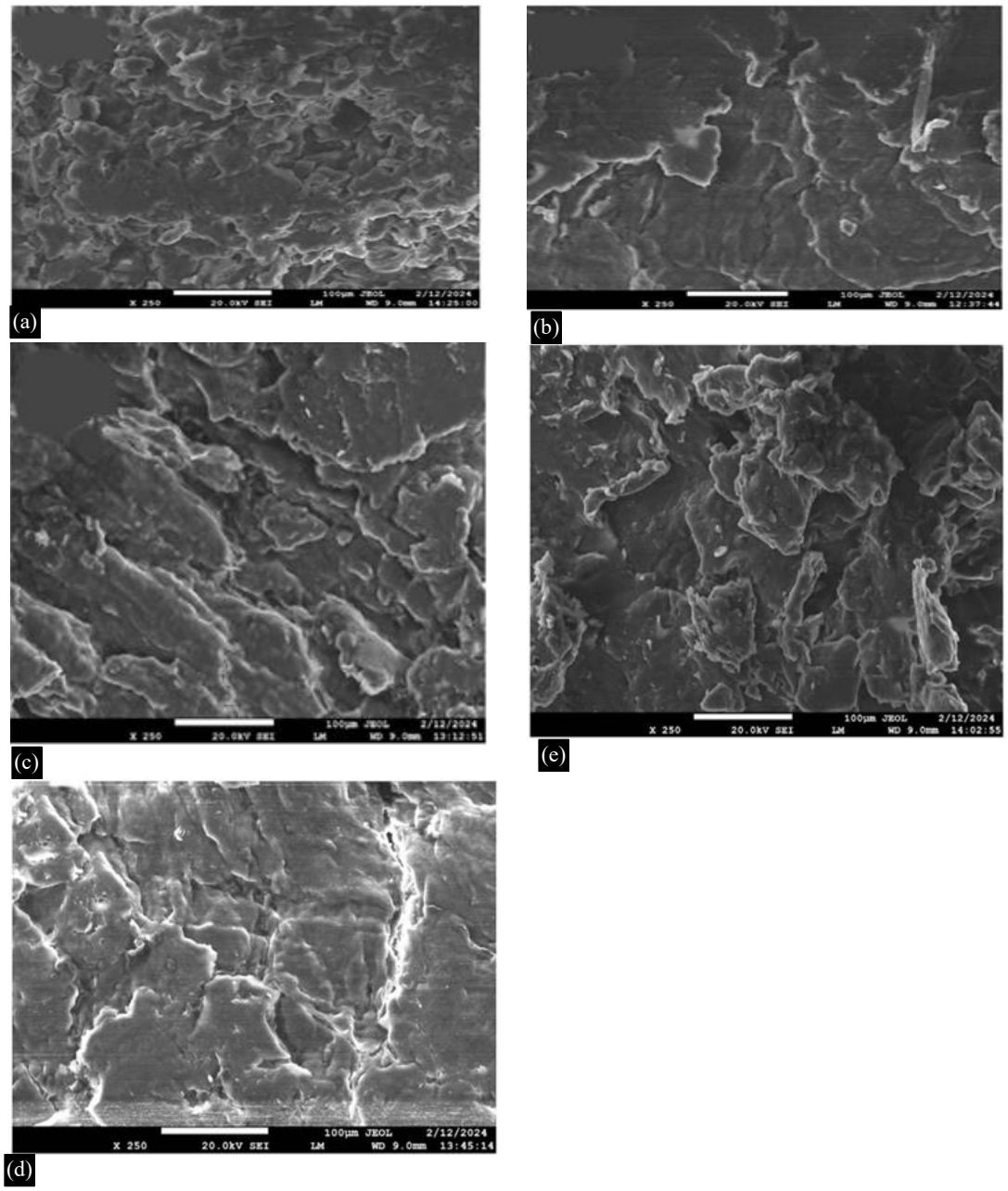


**Figure 10.** FESEM Images of PW and AFG-Based PW Composites at Different Concentrations: (a) pure PW (b) 0.20 Vol % (c) 0.40 Vol % (d) 0.80 Vol % (e) 1.60 Vol %

**Analysis of Thermal Conductivity of PW and AFG-Based Composites**

The thermal conductivity (k) of pure PW and its composites reinforced with AFG was experimentally measured using the Transient Plane Source (TPS) technique. Pure PW served as the baseline material, exhibiting a thermal conductivity of 0.265 W/m·K, as presented in Table 3 and graphically illustrated in Figure 11.

A progressive enhancement in thermal conductivity was observed with increasing AFG concentrations. At 0.20 vol%, the thermal conductivity increased to 0.301 W/m·K, showing a 13.58% improvement. This enhancement is attributed to the initial formation of thermally conductive pathways created by dispersed AFG nanoparticles. When the concentration was raised to 0.40 vol%, thermal conductivity rose to 0.322 W/m·K, marking a 21.51% increase over pure PW. The improvement at this stage is due to better dispersion and network formation, enabling more effective phonon transport.

 

The trend continued at 0.80 vol%, where the thermal conductivity reached 0.348 W/m·K, representing a 31.32% enhancement, indicating an increasingly interconnected thermal conduction network within the PCM matrix. The most significant improvement was recorded at 1.60 vol%, achieving a thermal conductivity of 0.388 W/m·K, which corresponds to a 46.42% increase compared to pure PW. This considerable improvement is linked to the development of a dense and continuous AFG network that facilitates efficient heat transfer [16].

These findings confirm that the incorporation of AFG significantly improves the thermal conductivity of PW. While lower to higher nanomaterial concentration (0.20–1.60 vol%) promote steady conductivity enhancement through improved dispersion and network formation, the highest value at 1.60 vol% reflects the formation of highly interconnected thermal pathways. However, it should be noted that excessive AFG may lead to nanoparticle agglomeration, which could introduce localized thermal resistance. Therefore, the optimal balance between thermal enhancement and microstructural stability should be carefully considered for practical applications in TESS.

**TGA of PW and AFG-Based Composites**

TGA was conducted to evaluate the thermal stability and decomposition characteristics of pure PW and AFG-reinforced PW composites. The TGA curves are presented in Figure 12, illustrating the weight loss behaviour of each sample under increasing temperature conditions.

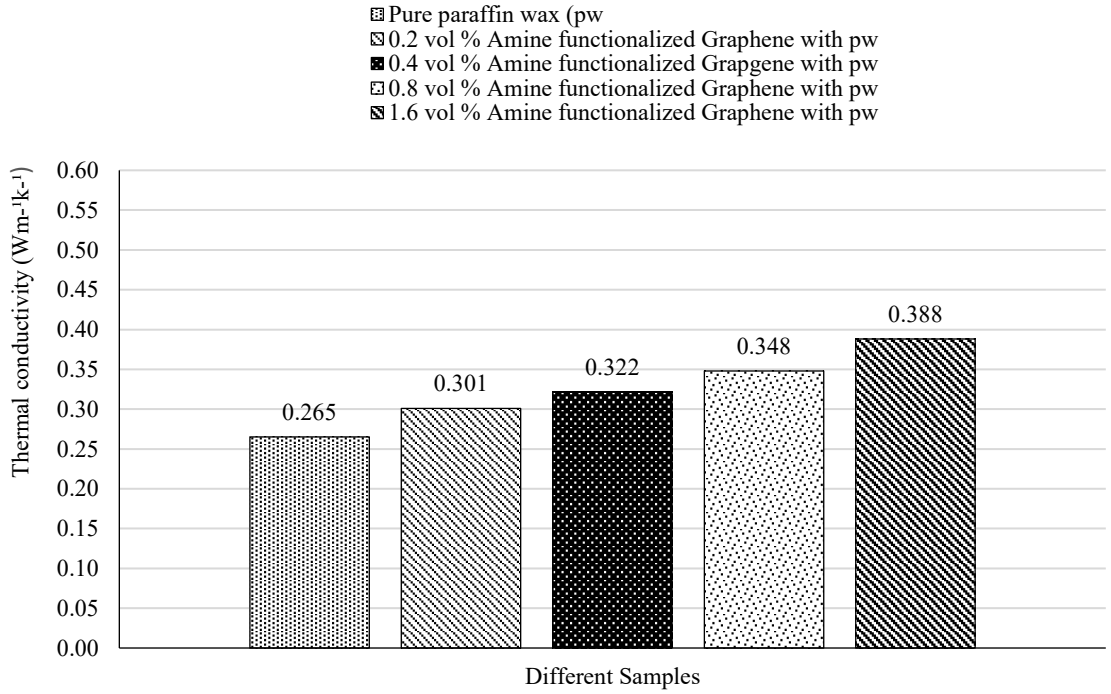


**Figure 11.** Thermal conductivity variation of PW and AFG-based PW composites at different concentrations.

**Table 3.** Thermal conductivity values of different samples (TPS method).

| Type of sample | Thermal conductivity, k (W/mK) |
|---|---|
| PW | 0.265 |
| 0.2 vol% AFG with PW | 0.301 |
| 0.4 vol% AFG with PW | 0.322 |
| 0.8 vol% AFG with PW | 0.348 |
| 1.6 vol% AFG with PW | 0.388 |

 

For pure PW, thermal degradation begins at approximately 250°C, followed by rapid mass loss, indicating low thermal resistance. In contrast, the addition of AFG significantly shifts the decomposition onset to higher temperatures, suggesting enhanced thermal stability. Specifically, the onset of decomposition for 0.80 vol% and 1.60 vol% AFG composites is delayed to the 280–290°C range, highlighting the improved heat tolerance of the modified PCM.

Additionally, the residual mass at 600°C provides further insight into the material's resistance to complete decomposition. Pure PW shows nearly total degradation with negligible residue, while AFG composites retain increasing amounts of residual weight as the concentration of AFG increases. The 1.60 vol% sample retains the highest residue (~7–8%), attributed to the inherent thermal stability of graphene nanosheets acting as a reinforcing framework that resists oxidative breakdown.

The primary decomposition temperature window also shifts with higher AFG concentration. Notably, the 1.60 vol% AFG composite exhibits major weight loss between 360–400°C, further affirming its enhanced thermal resistance. These results confirm that AFG effectively increases the thermal degradation threshold and structural integrity of the composite PCM.

Among all tested concentrations, 0.80 vol% AFG demonstrates an optimal balance delivering enhanced thermal resistance without excessive material retention or possible drawbacks such as nanoparticle agglomeration, which may occur at higher concentrations like 1.60 vol% and affect performance consistency.

**DSC Analysis of PW and AFG-based Composites**

The DSC thermograms of pure PW and its composites with varying concentrations of AFG are presented in Figure 13. These plots provide important information about the phase transition behavior, including melting temperature and enthalpy changes, which are vital parameters for thermal energy storage materials.

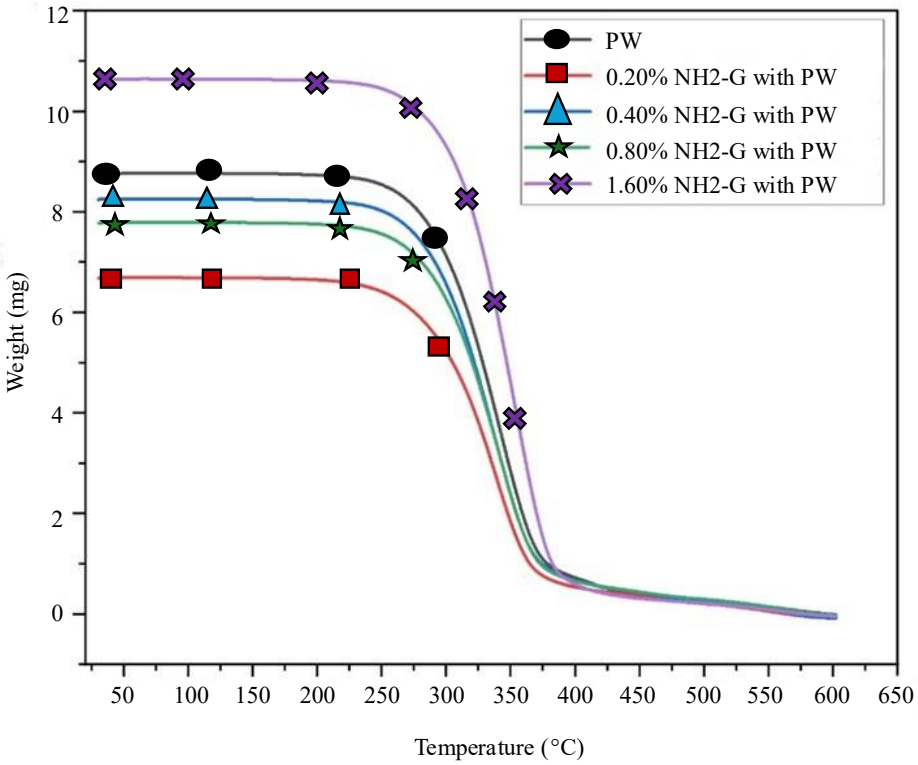


**Figure 12.** TGA profile of pure PW and AFG-based PW composites at various concentrations.

 

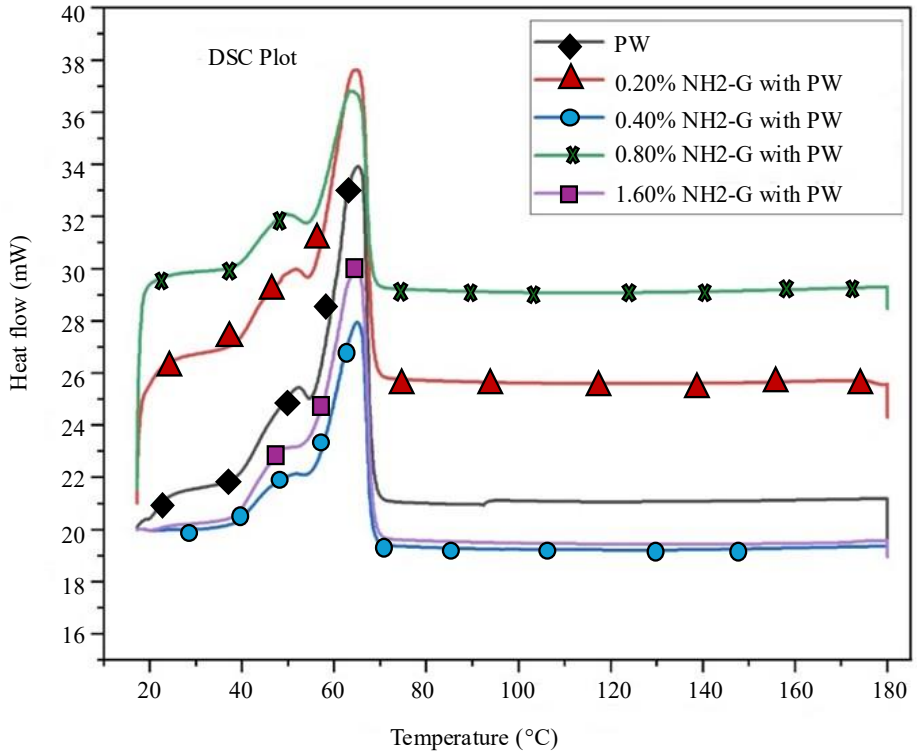


**Figure 13.** DSC Plot showing phase transition characteristics of Pure PW and AFG-Based PW composites.

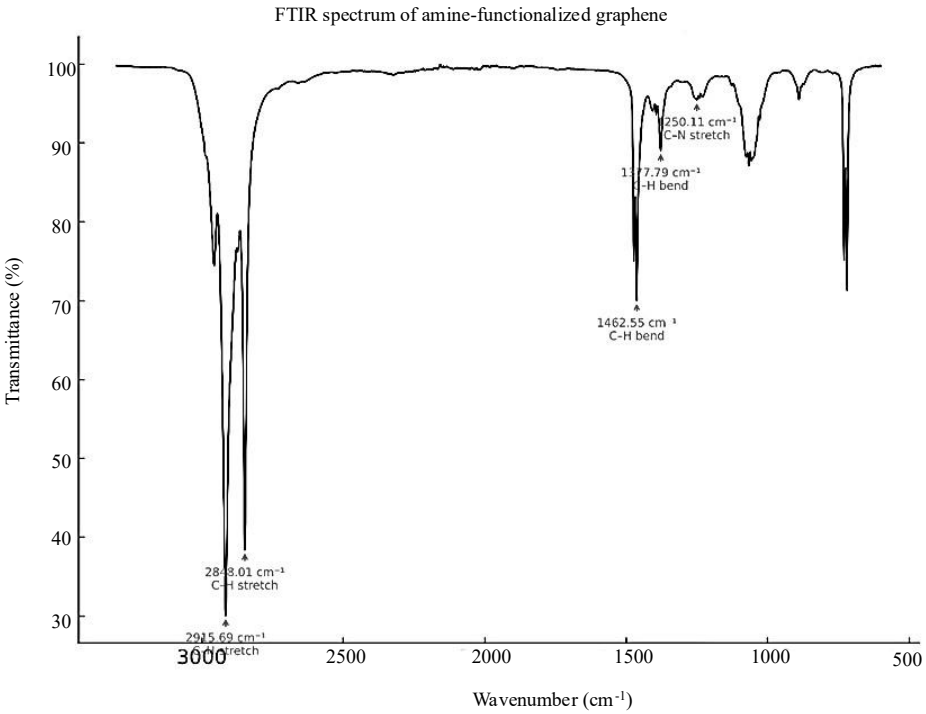


**Figure 14.** FTIR spectrum of amine-functionalized graphene (AFG) showing characteristic peaks of amine groups and other functional moieties.

The DSC curves reveal distinct endothermic peaks corresponding to the melting of PW and its AFG composites. A slight shift in melting temperatures is observed with increasing AFG content, which indicates molecular-level interactions between the paraffin matrix and the graphene additive. These

 

interactions influence the crystallization behavior, leading to enhanced heat transfer mechanisms within the composite structure.

The peak intensity increases notably for higher AFG concentrations (0.80 vol% and 1.60 vol%), suggesting an improved heat absorption rate and enhanced thermal conductivity. Additionally, the broadening of melting peaks in AFG reinforced PW indicates a more gradual phase transition. This effect is associated with enhanced thermal stability and more uniform heat distribution throughout the material.

However, as the concentration of AFG increases, a reduction in phase change enthalpy is observed. This decrease implies a reduction in latent heat storage capacity, possibly due to the partial replacement of PW by the additive. Despite this trade-off, the improved thermal conductivity of AFG compensates by enabling faster thermal response and more efficient energy transfer during phase transitions.

Overall, the DSC results affirm that incorporating AFG modifies the thermal behavior of PW composites, making them suitable for applications where rapid heat absorption and release are required.

**FTIR Analysis for Confirmation of Amine Functionalization**

The FTIR spectrum of AFG was obtained to verify the presence of amine groups and assess their potential role in enhancing compatibility with the PW matrix. As shown in Figure 14, the spectrum exhibits distinct absorption peaks at 2915.69 $cm^{-1}$ and 2848.01 $cm^{-1}$, corresponding to asymmetric and symmetric C–H stretching vibrations, respectively. Peaks at 1462.55 $cm^{-1}$ and 1377.79 $cm^{-1}$ are attributed to C–H bending modes, while the band at 1250.11 $cm^{-1}$ is associated with C–N stretching vibrations of amine groups. The presence of these functional groups is consistent with the supplier-provided amine functionalization process, which improves the wettability of graphene, strengthens interfacial bonding, and promotes homogeneous dispersion within the PW matrix. These chemical interactions are expected to contribute to the improved thermal conductivity and latent heat retention observed in the composite PCM.

## CONCLUSIONS

This experimental study presents a comprehensive evaluation of the thermal performance of PW composites reinforced with amine functionalized graphene for thermal energy storage applications. Experimental results demonstrate that the integration of AFG into PW significantly enhances its thermal conductivity, phase change characteristics, and overall heat retention capacity. The effects of nanoparticle concentration and HTF flow rate were systematically investigated to optimize both charging and discharging behavior. Based on the experimental findings, the following conclusions were drawn:

1. *Thermal charging and discharging behavior*: Increasing AFG concentration in PW reduces charging duration due to improved thermal conductivity, while discharging time increases owing to enhanced thermal storage capacity. This dual behavior supports effective heat absorption and delayed release.
2. *Optimal concentration identified*: A concentration of 0.80 vol% AFG was found to offer the most balanced thermal performance, reducing charging time by up to 61.5% and extending discharging time by 62.5% compared to pure PW. This concentration ensures good dispersion, optimal thermal pathways, and stable performance.
3. *Effect of agglomeration at higher concentration*: At 1.60 vol% AFG, agglomeration effects become apparent, restricting uniform dispersion and diminishing the enhancement in thermal performance. This leads to a plateau or slight increase in charging time and a reduction in discharging duration.
4. *Influence of flow rate*: The HTF flow rate plays a pivotal role in heat transfer of the system. Higher flow rates significantly enhance heat transfer, reducing both charging and discharging durations, while lower flow rates emphasize storage, extending both processes.
5. *Thermal conductivity enhancement*: The addition of AFG resulted in a progressive increase in thermal conductivity, reaching a maximum improvement of 46.42% at 1.60 vol%, as confirmed by TPS measurements. This improvement substantiates the role of graphene as an effective thermal conductivity enhancer in phase change systems.

 

6. *Thermal stability (TGA analysis):* TGA results revealed that AFG incorporation elevates the decomposition temperature and enhances thermal resistance. The composite with 0.80 vol% AFG exhibited optimal thermal stability, balancing structural integrity with thermal performance.
7. *Phase change behavior (DSC analysis):* DSC analysis confirmed improved thermal response with AFG addition. Shifts in melting temperature and peak broadening indicated modified crystallization behavior and enhanced heat absorption. The reduced latent heat was offset by improved thermal conductivity, making the composite suitable for rapid energy storage and release.

In conclusion, AFG reinforced PW composites demonstrate significant potential as advanced PCMs for TESS. Among all tested concentrations, 0.80 vol% AFG emerged as the most effective composition, offering superior thermal conductivity, efficient energy charging, extended discharging, and improved thermal stability -key attributes for next-generation TES applications in polymer composite-based systems.

## Conflict of Interest

The authors declare that there is no known conflict of interest or personal relationships that could have appeared to influence the work reported in this article.

## Data Availability Statement

The authors confirm that the data supporting the findings of this study are available within the article. Raw data that supports the findings of this study are available from the corresponding author, upon reasonable request.

## Funding Statement

The authors received no financial support for this article's research, authorship, and/or publication.

## Credit Authorship Contribution Statement

Daya Shankar Prasad: Methodology; Performed the experiments; Investigation; Data Curation; Validation; Writing first draft.

Pradeep Kumar Singh: Conceptualization; Formal Analysis; Validation; Resources; Planned and supervised the experiments; Finalizing the manuscript.

## Acknowledgements

The authors would like to acknowledge their appreciation and gratitude to Solar Energy Research Centre (SERC), Department of Mechanical Engineering, GLA University, Mathura, (U.P.)-281406, India to conduct experimental work. The authors also gratefully acknowledge the Advanced Centre for Materials Science (ACMS), IIT Kanpur, for facilitating the characterization of the samples.

## Nomenclature

| Symbol | Description | Unit |
|---|---|---|
| T | Temperature | °C |
| K | Thermal conductivity | $Wm^{-1}K^{-1}$ |
| P | Density | $Kgm^{-3}$ |
| $C_p$ | Specific heat capacity | $Jkg^{-1}K^{-1}$ |
| TESS | Thermal energy storage system | - |
| PCMs | Phase change materials | - |
| HTF | Heat transfer fluid | - |
| AFG | Amine-functionalized graphene | - |
| PW | Paraffin wax | - |
| DSC | Differential scanning calorimetry | - |
| TGA | Thermogravimetric analysis | - |
| FESEM | Field emission scanning electron microscopy | - |
| FTIR | Fourier Transform Infrared Spectroscopy | - |

 

## REFERENCES

1. Sharma A, Tyagi VV, Chen CR, Buddhi D. Review on thermal energy storage with phase change materials and applications. Renew Sustain Energy Rev. 2009;13(2):318-345. doi:10.1016/j.rser.2007.10.005.
2. Kuznik F, David D, Johannes K, Roux JJ. A review on phase change materials integrated in building walls. Renew Sustain Energy Rev. 2011;15(1):379-391. doi:10.1016/j.rser.2010.08.019.
3. Zhang H, Baeyens J, Cáceres G, Degrève J, Lv Y. Thermal energy storage: Recent developments and practical aspects. Prog Energy Combust Sci. 2016;53:1-40. doi:10.1016/j.pecs.2015.10.003.
4. Nedjem K, Teggar M, Hadibi T, Benkherouf A. Hybrid thermal performance enhancement of shell and tube latent heat thermal energy storage using nano-additives and metal foam. J Energy Storage. 2021;44:103347. doi:10.1016/j.est.2021.103347.
5. Agyenim F, Hewitt N, Eames P, Smyth M. A review of materials, heat transfer, and phase change problem formulation for latent heat thermal energy storage systems (LHTESS). Renew Sustain Energy Rev. 2010;14(2):615-628. doi:10.1016/j.rser.2009.10.015.
6. Khodadadi JM, Hosseinizadeh SF. Nanoparticle-enhanced phase change materials (NEPCM) with great potential for improved thermal energy storage. Int Commun Heat Mass Transf. 2007;34(5):534-543. doi:10.1016/j.icheatmasstransfer.2007.02.005.
7. Zhou D, Zhao CY, Tian Y. Review on thermal energy storage with phase change materials (PCMs) in building applications. Appl Energy. 2012;92:593-605. doi:10.1016/j.apenergy.2011.08.025.
8. Farid MM, Khudhair AM, Razack SA, Al-Hallaj S. A review on phase change energy storage: materials and applications. Energy Convers Manag. 2004;45(9-10):1597-1615. doi:10.1016/j.enconman.2003.09.015.
9. Cabeza LF, Castell A, Barreneche C, de Gracia A, Fernández AI. Materials used as PCM in thermal energy storage in buildings: A review. Renew Sustain Energy Rev. 2011;15(3):1675-1695. doi:10.1016/j.rser.2010.11.018.
10. Sharma RK, Ganesan P, Tyagi VV, Metselaar HSC, Sandaran SC. Developments in organic solid–liquid phase change materials and their applications in thermal energy storage. Energy Convers Manag. 2015;95:193-228. doi:10.1016/j.enconman.2015.01.084.
11. Sun X, Liu L, Mo Y, Yang S, Li Z. Enhanced thermal energy storage of a paraffin-based phase change material (PCM) using nano carbons. Appl Therm Eng. 2020;178:115992. doi:10.1016/j.applthermaleng.2020.115992.
12. Ermis K, Findik F. Thermal energy storage: A review article on thermal energy storage. Sustain Eng Innov. 2020;2(2):66-88. doi:10.37868/sei.v2i2.115.
13. Tao YB, He YL. A review of phase change material and performance enhancement method for latent heat storage system. Renew Sustain Energy Rev. 2018;93:245-259. doi:10.1016/j.rser.2018.05.028.
14. Singh RP, Kaushik SC, Rakshit D. Performance evaluation of charging process in a cascade latent heat storage system (C-LHSS) based on heat flux DSC results. Int J Therm Sci. 2020;151:106274. doi:10.1016/j.ijthermalsci.2020.106274.
15. Sarbu I, Dorca A. Review on heat transfer analysis in thermal energy storage using latent heat storage systems and phase change materials. Int J Energy Res. 2019;43:29-64. doi:10.1002/er.4196.
16. Prasad DS, Singh PK. Thermal charging-discharging analysis of PCM cylinder for amine-functionalized MWCNT-doped paraffin wax as a phase change material. Eng Res Express. 2025;7(1):015001. doi:10.1088/2631-8695/adb127.
17. He L, Wang H, Zhu H, Chen C, Zhang J. Thermal properties of PEG/graphene nanoplatelets (GNPs) composite phase change materials with enhanced thermal conductivity and photo-thermal performance. Appl Sci. 2018;8(12):2613. doi:10.3390/app8122613.
18. Khezri A, Sahebi M, Mohammadi M. Fabrication and thermal properties of graphene nanoplatelet-enhanced phase change materials based on paraffin encapsulated by melamine–formaldehyde. J Therm Anal Calorim. 2022;147(14):7683-7691. doi:10.1007/s10973-021-11085-7.
19. Singh PK, Nagar S, Singh M. Experimental analysis of thermal efficiency of functionalized graphene (COOH) reinforced PCM for thermal energy storage system. IOP Conf Ser Mater Sci Eng. 2021;1116(1):012008. doi:10.1088/1757-899X/1116/1/012008.

 

20. Nair AM, Naidu PVK. Comparison of charging and discharging period analysis of phase change materials-paraffin wax and myristic acid. Int J Curr Eng Technol. 2018;8(1):10886. doi:10.14741/ijcet.v8i01.10886.
21. Kanimozhi B, Harish K, Tarun BS, Kumar S. Charging and discharging processes of thermal energy storage system using phase change materials. IOP Conf Ser Mater Sci Eng. 2017;197:012040. doi:10.1088/1757-899X/197/1/012040.
22. Liu X, Rao Z. Experimental study on the thermal performance of graphene and exfoliated graphite sheet for thermal energy storage phase change material. Thermochim Acta. 2017;647:15-21. doi:10.1016/j.tca.2016.11.010.
23. Kumar P, Singh PK, Nagar S. Effect of different concentration of functionalized graphene on charging time reduction in thermal energy storage system. Mater Today Proc. 2021;44:146-152. doi:10.1016/j.matpr.2020.08.548.
24. Hosseini SM, Ghaffari M, Kahsari SM, Abbasi A. A study on nano-graphene oxide surface modification for the design of paraffin/graphene oxide phase change material. J Energy Storage. 2024;101:113738. doi:10.1016/j.est.2024.113738.
25. Kumar A, Gupta A, Sharma K, Verma N. Effect of graphene oxide on thermal charging and discharging behaviour of paraffin wax as nano-enhanced phase change materials. MRS Adv. 2024;9:1-6. doi:10.1557/s43580-024-00895-0.
26. Zhao Q, He F, Zhang Q, Huang J, Wang X. Microencapsulated phase change materials based on graphene Pickering emulsion for light-to-thermal energy conversion and management. Sol Energy Mater Sol Cells. 2019;203:110204. doi:10.1016/j.solmat.2019.110204.
27. Hussain A, Abidi IH, Tso CY, Chao CYH. Thermal management of lithium-ion batteries using graphene coated nickel foam saturated with phase change materials. Int J Therm Sci. 2018;124:23-35. doi:10.1016/j.ijthermalsci.2017.09.019.
28. Nagar S, Sharma K, Singh M, Gupta V. Charging analysis and characterizations of COOH group functionalized graphene combined with paraffin wax as phase change material for thermal energy storage applications. J Therm Anal Calorim. 2022;149:7505-7516. doi:10.1007/s10973-022-11365-w.
29. Viswanathan S, Antony Arockiaraj G, Kalam M, Krishnan V. Enhancement of quick charging and discharging of TES system by PCM mixed with Al2O3 nanoparticles for EV. Therm Sci. 2024;28(1):189-196. doi:10.2298/TSCI221126269V.
30. Lin Y, Jia Y, Alva G, Fang G. Review on thermal conductivity enhancement, thermal properties and applications of phase change materials in thermal energy storage. Renew Sustain Energy Rev. 2018;82:2730-2742. doi:10.1016/j.rser.2017.10.002.
31. Kalbande VP, Fating G, Mohan M, Patel A. Experimental and theoretical study for suitability of hybrid nano-enhanced phase change material for thermal energy storage applications. J Energy Storage. 2022;51:104431. doi:10.1016/j.est.2022.104431.
32. Etesami M, Nguyen MT, Yonezawa T, Lee JS. 3D carbon nanotubes-graphene hybrids for energy conversion and storage applications. Chem Eng J. 2022;446:137190. doi:10.1016/j.cej.2022.137190.
33. Mishra RK, Verma K, Mishra V, Prakash R. A review on carbon-based phase change materials for thermal energy storage. J Energy Storage. 2022;50:104166. doi:10.1016/j.est.2022.104166.
34. Putra N, Rawi S, Amin M, Sandi H. Preparation of beeswax/multi-walled carbon nanotubes as novel shape-stable nanocomposite phase-change material for thermal energy storage. J Energy Storage. 2019;21:32-39. doi:10.1016/j.est.2018.11.007.
35. Mayilvelnathan V, Arasu AV. Experimental investigation on thermal behavior of graphene dispersed erythritol PCM in a shell and helical tube latent energy storage system. Int J Therm Sci. 2020;155:106446. doi:10.1016/j.ijthermalsci.2020.106446.

 